Dimensional reductions from 2-D $Nb_4P_2S_{21}$ to 1-D ANb_2PS_{10} (A = Na, K, Rb, Cs, Tl) and to 0-D $Tl_5[Nb_2S_4Cl_8]Cl$ using halide molten salts

Hyunjin Bang, Youngmee Kim, Seri Kim, Sung-Jin Kim *

Division of Nanosciences, Ewha Womans University, Seoul 120-750, Korea

ARTICLE INFO

ABSTRACT

We found new synthetic routes to obtain 1-D quaternary thiophosphate compounds and a 0-D molecular complex containing a Nb_2S_4 core from a 2-D ternary thiophosphate, $Nb_4P_2S_{21}$. When $Nb_4P_2S_{21}$ was reacted with alkali metal halides (ACl; A = Na, K, Rb, Cs) or TlCl at 500–700 °C, the –S–S–S– bridges in 2-D Nb_2PS_{10}-S-$S_{10}PNb_2$ were excised to form a 1-D chain, and cations were inserted between the chains to form ANb_2PS_{10} (A = Na, K, Rb, Cs, Tl). We also found that thallium chloride (TlCl) is an excellent reagent for further excision, and it substitutes chloride ligands for the sulfur ligands of 2-D $Nb_4P_2S_{21}$ to form the molecular complex $Tl_5[Nb_2S_4Cl_8]Cl$. Crystal data for $TlNb_2PS_{10}$: monoclinic, Pn, a = 6.9452(11) Å, b = 7.3761(12) Å, 12.873(2) Å, β = 104.472(3)°, and Z = 2. Crystal data for $Tl_5[Nb_2S_4Cl_8]Cl$: orthorhombic, $Immm$, a = 7.001(5) Å, b = 9.509(7) Å, c = 15.546(11) Å, and Z = 2.

© 2008 Elsevier Inc. All rights reserved.

1. Introduction

The excision process has been one of the synthetic methods used to obtain novel building units from condensed solid state frameworks for new lattice engineered architectures [1–3]. Holm reported that $Re_6Q_8X_2$ (Q = S, Se; X = Cl) with a 3-D framework structure can be dimensionally reduced to a molecular compound, $[Re_6Q_8X_6]^{4-}$, by reacting it with M^IX (M = Cs, Tl; X = Cl) at high temperature (850 °C) [4,5]. The molten cyanides (NaCN or KCN) have also been used as excellent reagents for excising octahedral metal cluster cores from transition metal chalcogenides with polymeric framework structures [6–11]. Very recently, Yarovoi et al. [12] suggested molten KOH as a new excision reagent; a reaction between the polymeric compound $Re_6Q_8X_2$ (Q = S, Se; X = Br) and molten KOH results in the formation of $[Re_6 Q_8(OH)_6]^{n-}$ (Q = S, Se) cluster anions. These previous fruitful examples encourage us to apply the excision methodology to one of the niobium thiophosphate compounds, $Nb_4P_2S_{21}$, because it consists of Nb_2PS_{10} chains bridged by S_3^{2-} through PS_4^{3-} units, forming layers. We have expected to isolate niobium chalcogenide $[Nb_2S_4]^{4+}$ clusters or infinite niobium thiophosphate chains $[Nb_2PS_{10}]^{1-}$ from the 2-D framework by breaking the weak S–S interactions. Transition metal thiophosphates have been actively investigated due to their structural low dimensionality and importance as oxidizing host materials for secondary lithium batteries.

Here we report a new synthetic route to 1-D alkali metal or Tl containing quaternary thiophosphate compounds ANb_2PS_{10} (A = Na, K, Rb, Cs, Tl) starting from the 2-D $Nb_4P_2S_{21}$, and we also report a new soluble molecular compound, $Tl_5[Nb_2S_4Cl_8]Cl$, obtained by excising the $[Nb_2S_4]^{4+}$ cluster core from 2-D $Nb_4P_2S_{21}$ by reacting it with TlCl.

2. Experimental section

2.1. Synthesis

$Nb_4P_2S_{21}$ was prepared as described previously [13]. This compound was obtained by heating the high purity elements, Nb powder (Aldrich Chem. Co, −40 mesh, 99.9%), S powder (Sigma-aldrich, 99.98%) and P powder (Aldrich Chem. Co, 99.99%), in stoichiometric proportions in evacuated quartz tubes at 600 °C for eight days, followed by 10 h of cooling. This procedure yields deep-red needle crystals.

ANb_2PS_{10} (A = Na, K, Rb, Cs) was prepared by heating $Nb_4P_2S_{21}$ crystals with an excess amount of alkali metal halide (ACl; A = Na, K, Rb, Cs) in a $Nb_4P_2S_{21}$:ACl = 1:10 molar ratio. The reacting mixture was double-sealed in an evacuated quartz tube and heated at 700 °C for a week. Then, to obtain a good quality of single crystals, the heated product was slowly cooled to room temperature (3–4 °C/h). This process led to the formation of shiny dark-purple-red needle crystals. The crystals were stable in both air and moisture, and their structures were solved by X-ray crystallography. Previously, the same 1-D quaternary

Table 1
Comparisons of cell parameters for ANb_2PS_{10} (A = Na, K, Rb, Cs)

	$Nb_4P_2S_{21}$[a]	$NaNb_2PS_{10}$[b]	KNb_2PS_{10}[c]	$RbNb_2PS_{10}$[d]	$CsNb_2PS_{10}$[e]
Formula weight	1106.97	560.44	576.49	622.86	670.3
Crystal system	Monoclinic	Monoclinic	Orthorhombic	Monoclinic	Monoclinic
Space group	$C2/c$	$C2/c$	$Pca2_1$	Pn	Pc
Unit cell dimensions (Å)	$a = 26.055(3)$	$a = 25.979(2)$	$a = 12.974(3)$	$a = 7.083(2)$	$a = 14.040(3)$
	$b = 7.0546(8)$	$b = 7.500(5)$	$b = 7.4954(16)$	$b = 7.054(2)$	$b = 7.544(2)$
	$c = 13.017(1)$	$c = 13.017(9)$	$c = 13.279(3)$	$c = 12.727(3)$	$c = 12.972(3)$
	$\beta = 103.18(1)$	$\beta = 102.7(1)$		$\beta = 104.46(2)$	$\beta = 95.72(2)$
Volume(Å³)	2478(2)	2474.1(6)	1291.3(5)	655.0(3)	1367.0(5)

[a] Ref. [13].
[b] Ref. [15b].
[c] This work and Ref. [16].
[d] This work and Ref. [17].
[e] Ref. [18].

Table 2
Crystal data and structure refinement for $TlNb_2PS_{10}$ and $Tl_5[Nb_2S_4Cl_8]Cl$

	$TlNb_2PS_{10}$	$Tl_5[Nb_2S_4Cl_8]Cl$
Empirical formula	$Nb_2PS_{10}Tl$	$Cl_9\,Nb_2\,S_4\,Tl_5$
Formula weight	741.76	1654.96 g/mol
Temperature	293(2) K	293(2) K
Wavelength	0.71073 Å	0.71073 Å
Crystal system	Monoclinic	Orthorhombic
Space group	Pn	$Immm$
Unit cell dimensions	$a = 6.9452(12)$ Å	$a = 7.001(5)$ Å
	$b = 7.3761(12)$ Å	$b = 9.509(7)$ Å
	$c = 12.873(2)$ Å	$c = 15.546(11)$ Å
	$\alpha = 90.00°$	$\alpha = 90.00°$
	$\beta = 104.472(3)°$	$\beta = 90.00°$
	$\gamma = 90.00°$	$\gamma = 90.00°$
Volume	638.56(18) Å³	1034.9(13) Å³
Z	2	2
Density (calculated)	3.858 Mg/m³	5.311 Mg/m³
Absorption coefficient	16.064 mm⁻¹	41.395 mm⁻¹
F (000)	676	1408
Crystal size	$0.08 \times 0.03 \times 0.03$ mm³	$0.1 \times 0.5 \times 0.2$ mm³
Reflections collected	3373	2648
Independent reflections	1775 [R(int) = 0.0360]	547 [R(int) = 0.2183]
Data/restraints/parameters	1775/2/127	547/0/36
Goodness-of-fit on $F2$	1.072	0.977
Final R indices	$R_1 = 0.0288$,	$R_1 = 0.0542$,
[$I > 2sigma(I)$]	$wR_2 = 0.0628$	$wR_2 = 0.1156$
R indices (all data)	$R_1 = 0.0324$,	$R_1 = 0.0660$,
	$wR_2 = 0.0638$	$wR_2 = 0.1179$
Largest diff. peak and hole	0.935 and −1.442 e.Å⁻³	4.161 and −2.070 e.Å⁻³

thiophosphate compounds had been directly synthesized by reacting them with the stoichiometric ratios of four elements at high temperature (700 °C) [14–18]. $TlNb_2PS_{10}$ was prepared by heating $Nb_4P_2S_{21}$ with TlCl at a lower temperature, ∼500 °C, for a week. To obtain single crystals, the heated product was slowly cooled to room temperature (3–4 °C/h). This process led to the formation of shiny black needle crystals.

$Tl_5[Nb_2S_4Cl_8]Cl$ was obtained by heating $Nb_4P_2S_{21}$ and an excess amount TlCl in a 1:10 molar ratio at 700 °C for a week. Then single crystals were obtained by slow cooling to room temperature (3–4 °C/h). This process led to the formation of shiny dark-red chunk crystals that were unstable in the both air and moisture.

The powder X-ray diffraction (XRD) patterns were in good agreement with the simulated powder X-ray patterns from the single crystal coordinates of the known (ANb_2PS_{10}, A = Na, K, Rb, Cs) and the new ones ($TlNb_2PS_{10}$ and $Tl_5[Nb_2S_4Cl_8]Cl$).

The chemical compositions of the crystals were confirmed by an energy-dispersive X-ray (EDX) spectrometer equipped with an electron probe microanalyzer (EPMA; JXA-9600. EDX; linekeXL) for ANb_2PS_{10} (A = Na, K, Rb, Cs, T) and $Tl_5[Nb_2S_4Cl_8]Cl$.

2.2. Crystallography

Single crystal X-ray analyses were carried out on a SMART APEX diffractometer using Mo-$K\alpha$ radiation ($\lambda = 0.71071$ Å). The crystals were mounted on a glass fiber under epoxy. The CCD (charge coupled device) data were integrated and scaled using the SAINT PLUS and the structure was solved and refined by using SHEXTL V.5.1. The crystallographic data for $TlNb_2PS_{10}$ and $Tl_5[Nb_2S_4Cl_8]Cl$ are listed in Table 2, and selected bond lengths and angles are listed in Tables 3 and 4, respectively.

2.3. Micro Raman spectroscopy

Raman spectra of single crystals were measured at room temperature in a back scattering geometry using an Ar-ion laser line (514.5 nm) and a Kr-ion laser line (647.1 nm). The scattered light was analyzed by a triple spectrometer (Jobin Yvon T64000) equipped with a liquid-nitrogen cooled CCD detector. The laser beam was focused on a spot less than 2–3 μm in diameter using 100× Olympus lenses.

3. Results and discussion

We found new synthetic routes to obtain 1-D quaternary thiophosphate compounds ANb_2PS_{10} (A = Na, K, Rb, Cs, Tl) and a 0-D molecular complex $Tl_5[Nb_2S_4Cl_8]Cl$ by heating 2-D $Nb_4P_2S_{21}$ with halide molten salts as dimensional reducing agents. Previously, the same 1-D quaternary thiophosphate compounds were directly synthesized by reacting with the stoichiometric ratios of four elements at high temperature [14–18]. Also, Sokolov et al. [19] previously prepared $Cs_5[Nb_2S_4Cl_8]Cl$ containing $[Nb_2S_4Cl_8]^{4-}$ unit.

$Nb_4P_2S_{21}$ prepared by a direct solid state reaction was used as a starting material in these excision reactions. As shown in Fig. 1(a), $[Nb_2PS_{10}]$ chains are bridged by the S–S–S bond to form planes $[Nb_2PS_{10}$-S- $S_{10}PNb_2]$ parallel to the bc-plane. The S–S distances in the $[S_3^{2-}]$ units are 2.041(4) Å and 2.015(4) Å, implying the existence of true $[S_3^{2-}]$ catenated anions. Between the planes, only weak S–S van der Waals' interactions with 3.149–3.706 Å are found. Therefore, intercalation of molecules or ions between the layers would be possible. The repeating niobium clusters consist of double distorted bicapped trigonal prisms $[NbS_8]$ sharing a rectangular face and the infinite chains obtained by the biprisms'

Table 3
Selected bond lengths [Å] and angles [°] for TlNb$_2$PS$_{10}$

Nb–S	2.471(3)–2.644(3)	Nb–Nb	2.883(1), 3.769(6)
P–S	1.980(4)–2.080(4)	S–S	2.027(4)–2.056(4)
Tl–S	3.129(3)		
S(7)#1–Nb(1)–Nb(2)#1	55.11(7)	S(8)–Nb(2)–Nb(1)#2	55.19(7)
S(10)#1–Nb(1)–Nb(2)#1	55.36(7)	S(9)–Nb(2)–Nb(1)#2	55.74(7)
S(8)#1–Nb(1)–Nb(2)#1	54.04(7)	S(7)–Nb(2)–Nb(1)#2	54.13(7)
S(9)#1–Nb(1)–Nb(2)#1	54.07(7)	S(10)–Nb(2)–Nb(1)#2	54.30(7)
S(5)–Nb(1)–Nb(2)#1	134.57(7)	S(6)–Nb(2)–Nb(1)#2	119.84(7)
S(6)–Nb(1)–Nb(2)#1	119.10(7)	S(5)–Nb(2)–Nb(1)#2	132.62(7)
S(1)–Nb(1)–Nb(2)#1	115.23(8)	S(3)–Nb(2)–Nb(1)#2	110.37(8)
S(2)–Nb(1)–Nb(2)#1	136.54(7)	S(2)–Nb(2)–Nb(1)#2	139.94(6)

Symmetry transformations used to generate equivalent atoms: #1 $x-1/2, -y+1, z-1/2$ #2 $x+1/2, -y+1, z+1/2$.

Table 4
Selected bond lengths [Å] and angles [°] for Tl$_5$[Nb$_2$S$_4$Cl$_8$]Cl

Nb–Nb #4	2.906(6)	Tl(1)–Cl(1)	3.104(7)
Nb–Cl(1)	2.565(6)	Tl(2)–Cl(1) #1	3.104(7)
Nb–Cl(2)	2.527(6)	Tl(2)–Cl(1) #2	3.104(7)
Nb–S	2.505(6)	Tl(2)–Cl(1)	3.104(7)
S–S #4	1.980(15)	Tl(2)–Cl(1) #3	3.104(7)
Nb–Nb–Cl(1)	104.96(18)	Cl(2)#7–Nb–Cl(1)	79.07(14)
Nb–Nb–Cl(2)	137.30(14)	Cl(2)#7–Nb–Cl(2)	85.4(3)
Nb #4–Nb–S #4	54.55(10)	S #4–Nb–S #5	90.9(3)
Nb #4–Nb–S #5	54.55(10)	S #4–Nb–S #6	46.5(3)
Nb #4–Nb–S #6	54.55(10)	S #5–Nb–S #6	109.1(2)
Nb #4–Nb–S	54.55(10)	S #4–Nb–S	90.9(3)
Cl(1)#7–Nb–Cl(1)	150.1(4)	S #5–Nb–S	46.5(3)
Cl(2)–Nb–Cl(1)	79.07(14)	S #6–Nb–S	109.1(2)

Symmetry transformations used to generate equivalent atoms: #1 $x, y, -z$ #2 $-x, -y+1, z$ #3 $-x, -y+1, -z$ #4 $-x, -y, -z$ #5 $x, -y, z$ #6 $-x, y, -z$ #7 $-x, -y, z$.
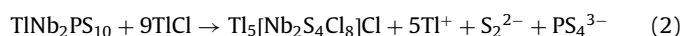
bonding through common S–S edges (Fig. 1(b)). Two such [Nb$_2$PS$_{10}$] chains are linked together by a sulfur atom, which forms a [S$_3$]$^{2-}$ group with the sulfur atom of both adjacent [PS$_4$]$^{3-}$ groups. When Nb$_4$P$_2$S$_{21}$ was reacted with an alkali metal halide flux (ACl; A = Na, K, Rb, Cs) at about 700 °C, 1-D chains of [Nb$_2$PS$_{10}$]$^{1-}$ were separated and alkali metal cations (A = Na, K, Rb, Cs) were inserted between chains (Fig. 2). The –S–S–S– bridges in Nb$_4$P$_2$S$_{21}$ turn into 2S^{2-} and S^0 to form 2[Nb$_2$PS$_{10}$]$^-$, according to the following reaction (1). After the reaction, the yellow sulfur powder was observed. When Nb$_4$P$_2$S$_{21}$ was reacted with TlCl at 700 °C, a molecular compound Tl$_5$[Nb$_2$S$_4$Cl$_8$]Cl was obtained; however, a TlNb$_2$PS$_{10}$ phase with an isostructure of RbNb$_2$PS$_{10}$ was obtained when Nb$_4$P$_2$S$_{21}$ was reacted with TlCl at 500 °C (Fig. 2(c)).

$$[\text{Nb}_2\text{PS}_{10}]-\text{S}-[\text{S}_{10}\text{PNb}_2] + 2A^+ \ (A = \text{Na, K, Rb, Cs, Tl}) \rightarrow 2A\text{Nb}_2\text{PS}_{10} + \text{S} \tag{1}$$
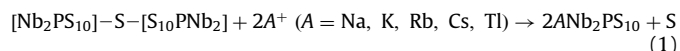
The ANb$_2$PS$_{10}$ (A = Na, K, Rb, Cs) structures commonly consist of 1-D $_\infty$[Nb$_2$PS$_{10}$]$^-$ chains, which are well separated by alkali metal cations. The crystallographic data for directly synthesized niobium thiophospate compounds, ANb$_2$PS$_{10}$ (A = Na, K, Rb, Cs), were previously reported [15–18]. The unit cell parameters on single crystals were in good agreement with previously reported structures of ANb$_2$PS$_{10}$ (A = Na [15b], K [16], Rb [17], Cs [18]) (Table 1). NaNb$_2$PS$_{10}$ could not be obtained as a single crystals with proper quality for single crystal diffraction study, but the powder XRD pattern was the same as that obtained from direct solid state reaction (see supporting information in Figure S1) [15b]. Basically the structures of ANb$_2$PS$_{10}$ prepared by direct solid structure reaction from four elements and by excision methodology starting from Nb$_4$P$_2$S$_{21}$ are the same. The quality of crystallographic data taken from the crystals obtained in this excision methodology was also equally good, except for NaNb$_2$PS$_{10}$. Along

the chains, the Nb$_2$S$_4^{4+}$ units are bridged by S$_2^{2-}$ and PS$_4^{3-}$ with the Nb–Nb distance range of 2.865(2)–2.891(1) Å indicating typical Nb^{4+}–Nb^{4+} bonding interactions. The distance of the P–S bonds is in the range of 2.084(6)–1.952(7) Å, which is in good agreement with the P^{5+}–S distance as shown in ternary phosphate compounds Nb$_4$P$_2$S$_{21}$. The charge balance of these compounds should be described by [A^+][Nb^{4+}]$_2$[P^{5+}][S$_2^{2-}$]$_3$[S^{2-}]$_4$ (A = Na, K, Rb, Cs, Tl). The overall structures of quaternary thiophosphates ANb$_2$PS$_{10}$ (A = Na, K, Rb, Cs) are closely related to Nb$_4$P$_2$S$_{21}$ and are similar to each other, except for cation positions between chains. In NaNb$_2$PS$_{10}$, instead of having the –S–S–S– bridges between chains as in Nb$_4$P$_2$S$_{21}$, Na$^+$ ions fill the spaces between chains [15b]. The arrangements of the anionic chains and cations in ANb$_2$PS$_{10}$ (A = K, Cs, Rb, Tl) differ from those of NaNb$_2$PS$_{10}$, but are similar to each other. In ANb$_2$PS$_{10}$ (A = K, Cs, Rb, Tl), A^+ cations fill every van der Waals' gap between chains. However, in NaNb$_2$PS$_{10}$, cations fill every other chain. Consequently, the unit cell dimension of NaNb$_2$PS$_{10}$ along the a-axis direction is double compared to the corresponding c-axis of KNb$_2$PS$_{10}$ and a-axis of CsNb$_2$PS$_{10}$. RbNb$_2$PS$_{10}$ and CsNb$_2$PS$_{10}$ have similar structures, but with different space symmetries. Raman spectra show the breaking of the –S–S–S– bond by metal halides (Fig. 4). The characteristic of –S–S–S– band appears at about 483 nm, with medium intensity, but the corresponding band disappears in ANb$_2$PS$_{10}$ (A = Na, K, Rb, Cs).

We also discovered that thallium chloride (TlCl) is an excellent reagent for isolating the [Nb$_2$S$_4$]$^{4+}$ core from a 2-D Nb$_4$P$_2$S$_{21}$ to yield a molecular compound, Tl$_5$[Nb$_2$S$_4$Cl$_8$]Cl, at high (~700 °C) temperatures. The reaction that takes place is described by the following reaction (2). In Tl$_5$[Nb$_2$S$_4$Cl$_8$]Cl, the [Nb$_2$S$_4$]$^{4+}$ core consisting of a short Nb$^\chi$–Nb$^\chi$ pair with two S$_2^{2-}$ units in between remains; and the S$_2^{2-}$ and PS$_4^{3-}$ units bridging two neighboring [Nb$_2$S$_4$]$^{4+}$ cores are replaced by Cl$^-$, forming [Nb$_2$S$_4$Cl$_8$]$^{4-}$ in the following reaction (2).

$$\text{TlNb}_2\text{PS}_{10} + 9\text{TlCl} \rightarrow \text{Tl}_5[\text{Nb}_2\text{S}_4\text{Cl}_8]\text{Cl} + 5\text{Tl}^+ + \text{S}_2^{2-} + \text{PS}_4^{3-} \tag{2}$$

This molecular complex, Tl$_5$[Nb$_2$S$_4$Cl$_8$]Cl, is soluble in a polar solvent; therefore, it can be used as a building block to construct a new family of compounds. This compound has an isostructure of a previously reported Cs$_5$[Nb$_2$S$_4$Cl$_8$]Cl that contains [Nb$_2$S$_4$]$^{4+}$ core with crystallographic symmetry of *Immm* [19]. In the previous study, K$_4$[Nb$_2$(S$_2$)$_2$(NCS)$_8$] was obtained starting from a layered compound (NbS$_2$Cl$_2$)$_x$ by reacting it with KSCN at 180 °C. In the reaction of K$_4$[Nb$_2$(S$_2$)$_2$(NCS)$_8$] with concentrated HCl, all the NCS ligands are replaced by chloride ligands to form [Nb$_2$S$_4$Cl$_8$]^4. Tl$_5$[Nb$_2$S$_4$Cl$_8$]Cl consists of [Nb$_2$(S$_2$)$_2$Cl$_8$]$^{4-}$ anions, Tl$^+$ cations, and isolated Cl$^-$ anions (Fig. 3). The [Nb$_2$(S$_2$)$_2$Cl$_8$]$^{4-}$ anions contain Nb$^\chi$–Nb$^\chi$ pairs with an Nb–Nb distance of 2.906(6) Å, which is not very different from the Nb–Nb distance of 2.871(1) Å found in Nb$_4$P$_2$S$_{21}$, indicating that the [Nb$_2$S$_4$]$^{4+}$ core remains intact. The
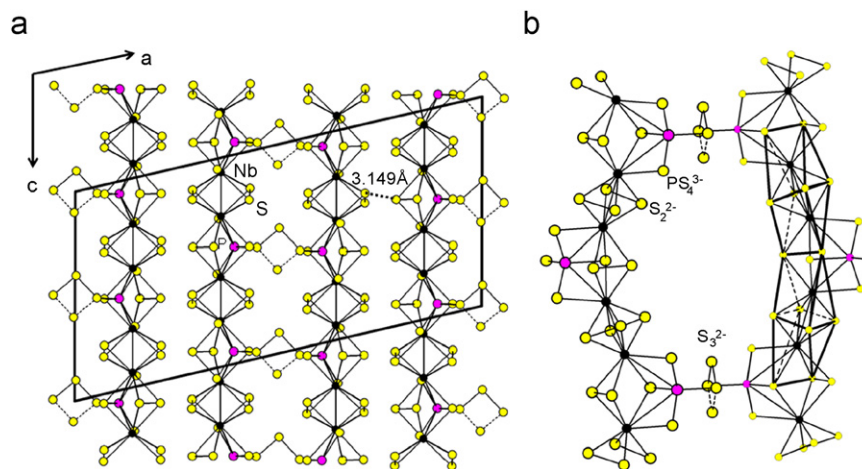
Fig. 1. (a) Structure of $Nb_4P_2S_{21}$ viewed along b-axis. (b) $[Nb_2PS_{10}]$ chains consisted of $[Nb_2S_{12}]$ and $[PS_4]$ units are bridges by S–S–S to form planes $[Nb_2PS_{10}$–S–$S_{10}PNb_2]$ parallel to the bc-plane. In the S–S–S unit, the S in the center is disordered over two sites with 50% occupancy; therefore only one out of two sites is connected as bonds by solid lines. Yellow circles are S atoms, small pink circles are P atoms and black circles are Nb atoms.
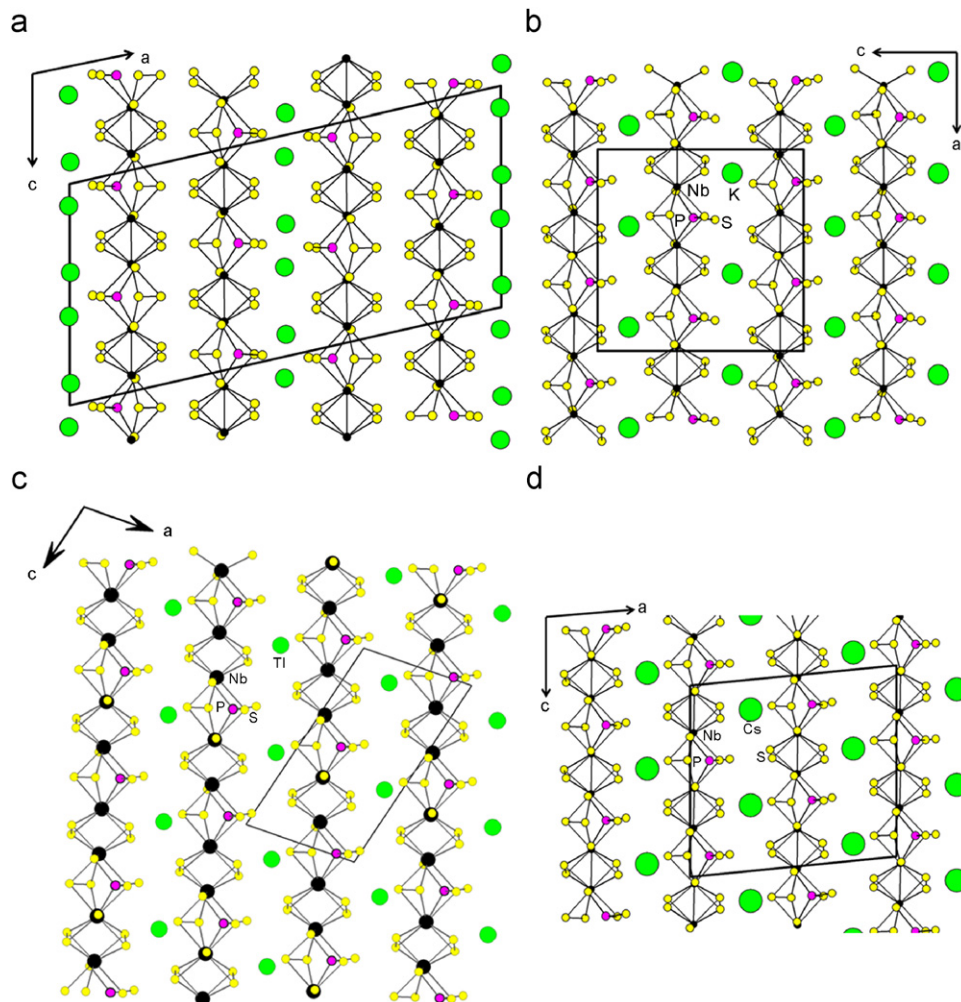

Fig. 2. (a) Structure of $NaNb_2PS_{10}$ viewed along b-axis. (b) Structure of KNb_2PS_{10} viewed along b-axis. (c) Structure of $TlNb_2PS_{10}$ viewed along b-axis. (d) Structure of $CsNb_2PS_{10}$ viewed along b-axis.

coordination geometry of the Nb atoms (if the Nb–Nb bond is disregarded) is a distorted square antiprism composed of 4S atoms and 4Cl atoms.

In summary, we have found new synthetic routes to obtain 1-D quaternary thiophosphate compounds and a 0-D molecular complex containing an $[Nb_2S_4]^{4+}$ core starting from a 2-D ternary

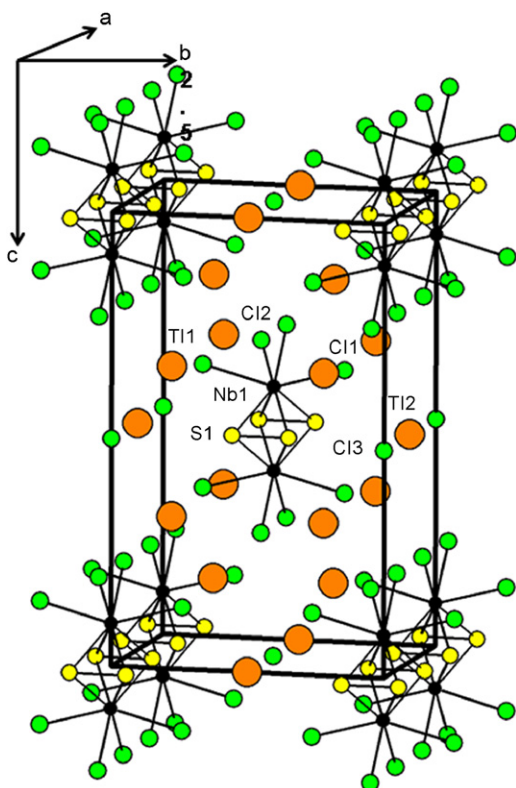**Fig. 3.** Structure of $Tl_5[Nb_2S_4Cl_8]Cl$. Small yellow circles are S atoms, small green circles are Cl atoms, black circles are Nb atoms, and large orange circles are Tl atoms.

crystal structure of ANb_2PS_{10} varies due to the different relative orientations of chains and cations depending on the cations' size. The crystal structures of a series of ANb_2PS_{10} and $Tl_5[Nb_2S_4Cl_8]Cl$ are the same whether they are synthesized by a direct solid state reaction or by the excision method. This excision methodology suggests that many more low-dimensional clusters or molecular building blocks can be obtained from classical solid state materials.

4. Supporting information

The crystallographic files in CIF format for the title compounds have been deposited with CSD numbers 417946, 417945, 417943, and 417942 for ANb_2PS_{10} ($A =$ K, Rb, Tl) and $Tl_5[Nb_2S_4Cl_8]Cl$, respectively.

Appendix A. Supplementary Materials

Supplementary data associated with this article can be found in the online version at doi:10.1016/j.jssc.2008.03.040.
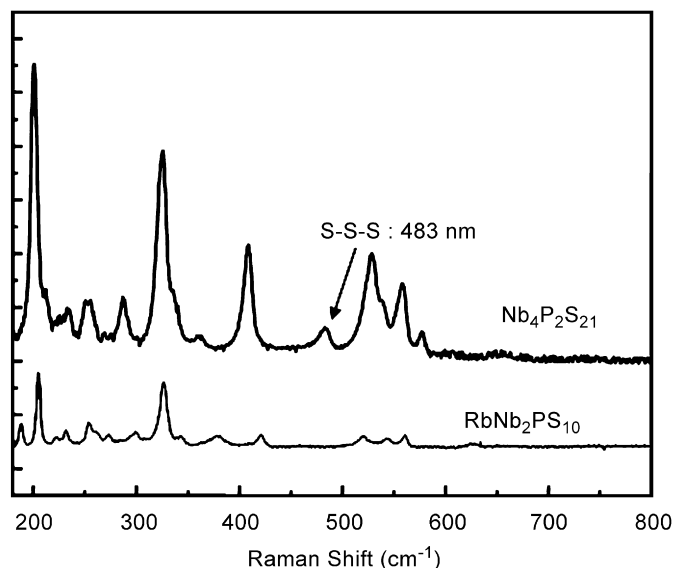

Fig. 4. Raman spectra of $Nb_4P_2S_{21}$ and $RbNb_2PS_{10}$: at 483 nm the –S–S–S– bond stretching band appears in $Nb_4P_2S_{21}$ and disappears in $RbNb_2PS_{10}$.

thiophosphate $Nb_4P_2S_{21}$. The reaction of 2-D ternary thiophosphate $Nb_4P_2S_{21}$ with metal halides excises the $_\infty[Nb_2PS_{10}^-]$ chains by breaking the S–S–S bridging and further excision resulting in an isolated $[Nb_2S_4]^{4+}$ core was observed. The symmetry of the

References

[1] Y. Kim, S.-M. Park, W. Nam, S.-J. Kim, Chem. Commun. (2001) 1470–1471.
[2] Y. Kim, S.-M. Park, S.-J. Kim, Inorg. Chem. Commun. 5 (2002) 592–595.
[3] M.V. Bennett, M.P. Shores, L.G. Beauvais, J.R. Long, J. Am. Chem. Soc. 122 (2000) 6664–6668.
[4] J.R. Long, A.S. Williamson, R.H. Holm, Angew. Chem. Int. Ed. Engl. 34 (1995) 226–229.
[5] E.G. Tulsky, J.R. Long, Inorg. Chem. 40 (2001) 6990–7002.
[6] Y.V. Mironov, A.V. Virovets, N.G. Naumov, V.N. Ikorskii, V.E. Fedorov, Chem. Eur. J. 6 (2000) 1361–1365.
[7] L.G. Beauvais, M.P. Shores, J.R. Long, J. Am. Chem. Soc. 122 (2000) 2763–2772.
[8] N.G. Naumov, A.V. Virovets, M.N. Solokov, S.B. Artemkina, V.E. Fedorov, Angew. Chem. Int. Ed. Engl. 37 (1998) 1943–1945.
[9] Y.V. Mironov, J.A. Cody, T.E. Albrecht-Schmitt, J.A. Ibers, J. Am. Chem. Soc. 119 (1997) 493–498.
[10] (a) M.P. Shores, L.G. Beauvais, J.R. Long, J. Am. Chem. Soc. 121 (1999) 775–779;
(b) M.P. Shores, L.G. Beauvais, J.R. Long, Inorg. Chem. 38 (1999) 1648–1649;
(c) L.G. Beauvais, M.P. Shores, J.R. Long, Chem. Mater. 10 (1998) 3783–3786.
[11] C. Magliocchi, X. Xie, T. Hughbanks, Inorg. Chem. 39 (2000) 5000–5001.
[12] S.S. Yarovoi, Y.V. Mironov, D.Y. Naumov, Y.V. Gatilov, S.G. Kozolva, S.-J. Kim, V.E. Fedorov, Eur. J. Inorg. Chem. (2005) 3945–3949.
[13] R. Brec, M. Evain, P. Grenouilleau, J. Rouxel, Rev. Chim. Min. t.20 (1983) 283–294.
[14] M.N. Sokolov, R. Hernandez-Molina, M.R.J. Elsegood, S.L. Heath, W. Clegg, A.G. Skyes, J. Chem Soc., Dalton Trans. (1997) 2059–2065.
[15] (a) S.-J. Kim, S. Yim, E.-Y. Goh, H. Kang, W. Kang, D. Jung, Chem. Mater. 15 (2003) 2266–2271;
(b) E.-Y. Goh, S.-J. Kim, D. Jung, J. Solid State Chem. 168 (2002) 119–125.
[16] J. Do, H. Yun, Inorg. Chem. 35 (1996) 3729–3730.
[17] C. Kim, H. Yun, Acta Crystallogr. C 58 (2002) i53–i54.
[18] J. Kwak, C. Kim, H. Yun, J. Do, Bull. Korean Chem. Soc. 28 (2007) 701–704.
[19] M. Sokolov, H. Imoto, T. Saito, V.E. Fedorov, Z. Anorg. Allg. Chem. 625 (1999) 989–993.